eJSE International

Special Issue: Electronic Journal of Structural Engineering 14(1) 2015

Pattern Recognition Based on Time Series Analysis Using Vibration Data for Structural Health Monitoring in Civil Structures

S. Mustapha
Department of Mechanical Engineering, American University of Beirut, Beirut, Lebanon
Infrastructure, Transport and Logistics, National ICT of Australia, Sydney, Australia

Y. Hu, K. Nguyen, M. Makki Alamdari & P. Runcie
Infrastructure, Transport and Logistics, National ICT of Australia, Sydney, Australia

U. Dackermann, V.V. Nguyen & J. Li
The Centre for Built Infrastructure Research, University of Technology, Sydney, Sydney, Australia

L.Ye
Centre for Advanced Materials Technology, The University of Sydney, Sydney, Australia

ABSTRACT: A statistical pattern recognition technique was developed based on the time series analysis to detect cracking in steel reinforced concrete structures using vibration measurements. The technique has been developed for the Sydney Harbour Bridge. The measurements were collected from single and tri-axial accelerometers, which were integrated into sensor nodes that were developed at the National ICT Australia.
The approach is based on two staged Auto-Regressive (AR) and Auto-Regressive with exogenous inputs (ARX) prediction models. The variation between the residual errors obtained from the intact and damaged states were used to define a Damage Index (DI) capable of identifying physical changed which could be due to structural damage. The effect of the severity of damage on the deviation of the AR-ARX model from its intact state was also scrutinised. The results of the field trial and the laboratory testing demonstrated the ability of the approach in identifying the presence of cracking and handling large volumes of data in a very efficient manner.

1 INTRODUCTION

Operational loading as well as extreme natural events and weather conditions on civil infrastructures made them susceptible to various types of structural damage, which may lead to disruption of the operation of the structure in some cases or may result in catastrophic failures if not detected at early stage and appropriate actions are taken. Structural Health Monitoring (SHM) systems have proven high proficiency for early detection and assessment of damage, in particular with the current advancement in sensing and hardware technology, which has made it a more feasible and reliable approach. SHM systems attracted the attention of many engineers and researchers working in the field as a revolutionary method to detect and assess damage during and after severe loading events (Mustapha et al. 2012). SHM help extend the life of assets by detecting damage before it becomes severe. In addition public safety is maintained, inspection productivity can be optimized and disruption to asset users is minimized (Silva et al. 2007).

Signal processing and damage feature extraction are fundamental aspects of any SHM system. This process usually involves the identification of features that are sensitive to damage from the collected data. This is then used as a damage "signature" that can be used to differentiate between intact and damaged structures (Fugate et al. 2001). The time series approach is based on signal analysis of measured data from single or multiple types of sensors, for instance acceleration or strain measurement data, and is highly capable to handle large volume of data. The concept of time series analysis was originally applied in the field of econometrics to investigate stock prices, production and interest rates, and later had much broader applications to include speech recognition, image analysis and DNA sequence analysis (Yao and Pakzad 2012). The main concept is that a time series model is fitted to a measured response from the system being monitored when the system is intact and the coefficients (or the residual error) of the model can be used as the damage-sensitive features. Data are then collected at a subsequent time and transformed using the time series model. If the input is known then any changes in the residual error indicate a change in the behaviour for the physical system – thus indicating potential damage to the structure. (Farrar and Worden 2012).

Many researchers have been working on time series analysis for the application in SHM for the last two decades. Hoon Sohn et al. (2001) used statistical pattern recognition techniques based on time series analysis of fiber optic strain gauge data obtained from two structural conditions of a high speed patrol boat. They used two-staged AR-ARX time series as well as outlier analysis with Mahalanobis distance measure to differentiate between data collected from different structural conditions. In addition, Sohn et al. (2001) applied time series analysis to localize damage in an 8 degrees of freedom mass-spring system which was also based on an AR-ARX model. The residual errors were used to define a damage indicator. Thanagasundram et al. (2006) focused on the detection of ball bearing faults in dry vacuum pumps using an autoregressive algorithm by monitoring the vibration spectra collected from the bearing elements at different loading speed and loading factors. Da Silva et al. (2007) focused on damage detection using AR-ARX model, the authors focused on the application of the fuzzy c-means clustering of damage indices in an unsupervised learning technique. Additional work was carried by Da Silva et al. (2008) used auto-regressive moving average with exogenous input (ARMAX) system identification model and statistical process control charts for linear prediction to detect and locate damage. The data used were collected using PZT patches bonded to a lightweight structure (aluminum beam). Further work was completed by Lautour et al. (2010) where they used an AR model to establish a damage sensitive feature of signals extract from a 3-storey bookshelf and phase II ASCE structure under dynamic excitation and then applied the ANNs for damage classification. Moreover, Peng et al. (2011) presented an integrated approach of the Nonlinear Auto-Regressive Moving Average with exogenous inputs (NARMAX) and the Nonlinear Output Frequency Response Functions (NOFRFs) to the detection of damage in engineering structures. Gul et al. (2011;2013) have also used time series analysis to detect, locate and assess the extent of the structural changes in a steel frame structure.

In this study, an AR and ARX are combined in a two-staged process to be used in the prediction of cracking in steel reinforced concrete structures. A Damage Index (DI) was defined based on the change in the residual errors calculated between the prediction and the measured data before and after damage occurs. Furthermore, the ability to detect and assess gradual cracking was investigated. Several challenges associated with the application of the proposed method, in the field, were investigated. The accuracy in the damage prediction of the two-staged AR-ARX model was assessed based on field trials on the iconic Sydney Harbor Bridge and through laboratory testing.

2 TIME SERIES ANALYSIS – PATTERN RECOGNITION

2.1 *Theoretical background*

Based on the theory of system dynamics, given that the input and the transfer function of the structure are known, then the output response from the structure can be predicted. However, in the case where the transfer function is unknown, the system is treated as a "black box" whose properties can be identified through the analysis of the system's inputs and outputs.

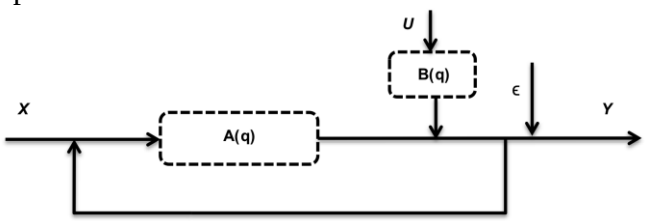

Figure 1. Block diagram for a typical dynamic system.

Figure 1 displays a block diagram of a dynamic system with feedback loop where X and Y are the input and the output of the system, respectively. A(q) represents the dynamic function of the system, B(q) is the disturbance function, q is the lag operator, U is the external excitation (which could be operational or environmental loading such as traffic loading and wind excitation) and ϵ is the measurement noise.

Base on that, the governing equation describing the system above can be built as shown in Equation (1):

$$Y = A(q)X + B(q)U + \epsilon \quad (1)$$

where the general polynomial equations $A(q)$ *and* $B(q)$ are written in terms of the time-shift operator q^{-1}.

$$A(q) = 1 + a_1 q^{-1} + a_2 q^{-2} + a_3 q^{-3} + \cdots + a_k q^{-k}$$
$$B(q) = b_1 q^{-1} + b_2 q^{-2} + b_3 q^{-3} + \cdots + b_k q^{-k}$$

The model order for $A(q)$ *and* $B(q)$ are considered to be non-zero, consequently ARX models are used (Gul and Catbas 2011). Furthermore, the negative exponent of q leads to the backshift when applied to a time series to calculate the previous element in the series.

For the time delay, Y can also be expressed as a function of X when the lag operator q is introduced, and then Equation 1 can be arranged as:

$$qX = A(q)X + B(q)U + \epsilon \quad (2)$$

Moving $A(q)X$ to the left side of Equation 2 and by extracting the homogeneity X, the standard expression of ARX model can be obtained as in Equation 3:

$$\Phi_{ARX}(q)X = \Theta(q)_{ARX}U + \epsilon \quad (3)$$

$\Phi_{ARX}(q)$ and $\Theta_{ARX}(q)$ are the two polynomials describing the ARX model, and ϵ is the residual error which should be Gaussian white noise with zero mean (De Lautour and Omenzetter 2010). When the residual error is not Gaussian distributed, the model requires further refinement to establish the system with the correct dynamic characteristics.

As the external input excitation into the system (U) is unknown, it is assumed that the error term (e) between the measured and the predicted responses from an AR model can be an estimate as the external input (Silva et al. 2007;Sohn et al. 2001). Note the resulting error (e) from the AR model could be very large due to the ambient excitation factors, including wind; seawater and traffic loading that are not included in the AR model. An AR model can be expressed as in Equation 4:

$$\Phi_{AR}(q)X = e \quad (4)$$

To determine the order of the model, there are several criterions that are widely used including the Akaike's information theoretic (AIC), the Akaike's final prediction error (FPE) and the Bayesian information criterion (BIC) (Brockwell and Davis 2002), in this work the AIC method was used to determine the order of AR model. The total order of the two polynomials in the ARX model should be smaller than that of AR model to avoid over-prediction. The coefficients of AR and ARX models are estimated using the Yule-Walker method (Brockwell and Davis 2002).

Occurrence of damage in the structure results in the change of the $\Phi(q)_{ARX}$ and $\Theta(q)_{ARX}$, consequently the data collected from the new condition of the structure (for instance with damage) cannot fit into the reference model, this form the basis of the concept adopted in this study.

2.2 *Damage Index*

After establishing the AR and the ARX models for the benchmark structure, the residual errors (ϵ_h - b corresponds to the benchmark) calculated could be obtained using any set of intact data. Similarly, for any unknown or structural damage conditions of the structure, the residual errors (ϵ_u - u corresponds to the unknown condition of the structure) can be also obtained using the ARX model developed earlier.

Following that, the ratio of the standard deviation of both residual errors (for benchmark and unknown conditions) can be used as damage sensitive feature. Therefore, the DI can be defined as (Sohn et al. 2001):

$$DI = \frac{\sigma(\epsilon_u)}{\sigma(\epsilon_h)} \quad (5)$$

where ϵ_u ad ϵ_h are the residual errors obtained from the benchmark and the unknown/damaged structures, respectively. σ denotes the standard deviation of the sequence.

Theoretically, when the DI is equal to 1, then the unknown condition matches the benchmark (no damage occurred); however when the ratio exceeds the value of 1 then this indicates a change in the structural condition of the structure. In reality there are many uncertainties that may deviate the value of DI from 1 for the healthy case, therefore it is critical to define a threshold in some cases to assess the structural health.

2.3 *Damage detection algorithm*

Before proceeding with the data analysis, the sample size required to build the AR-ARX model must be determined. An insufficient number of samples may lead only to partial modelling of the dynamic characteristic of the system, while too many samples may increase the uncertainty of the model prediction. Also, a larger sample size most likely results in over fitting, in other words, the AIC order selection method will select a much higher order. Empirical study was performed and resulted that a sample size between 500-700 sampling points (about 2 seconds of recording) should be satisfactory to give a precise prediction about the model for the current data.

The subsequent step is the standardization process. There are several factors which can influence the collected data including environmental conditions (e.g. humidity and temperature) as well as operational conditions (data collection), therefore it is essential to standardise the signals in order to eliminate any environmental and operational effects while maintaining features due to the change in structural conditions. The standardisation process is done by subtracting the mean from the original raw signal and dividing it by the standard deviation, as shown in Equation 6:

$$x = \frac{x_{raw} - \mu_x}{\sigma_x} \quad (6)$$

where x is the standardised time series of the original raw signal (x_{raw}), μ_x and σ_x are the mean and the standard deviation, respectively.

Following that, the AIC method was applied to determine the order of the AR model and the Yule Walker method was used to determine the coefficients for the benchmark structure. Later the ARX model was calculated (using the residual error terms from the AR model as an input) and the residual errors were obtained for the benchmark structure.

The residuals errors are also obtained from the structure with an unknown condition. At this stage the residual errors are now available for the benchmark and the unknown condition of the structure, an assessment is then carried out using the DI defined in Equation 5. The full process is summarised in Figure 2.

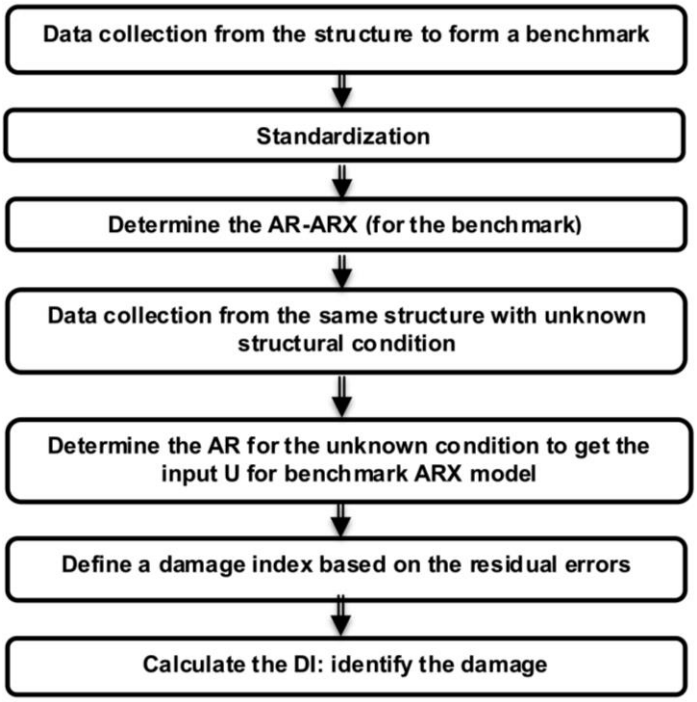

Figure 2. Flow chart for the damage identification algorithm.

3 EXPERIMENT SET-UP

For the validation of the AR-ARX model, two sets of data were used: (a) the first set of data was collected using a simplified section of the deck (on the bus lane) of the Sydney Harbour Bridge Structure, which was manufactured and tested in the laboratory and (b) the second set of data was directly obtained from sensors that are currently deployed on the Sydney Harbour Bridge.

For the data collection, the sensor node developed at the National ICT Australia was used. The node consists of a custom designed hardware circuit board, which is built around off-the-shelf ARM-based Gumstix "Overo" micro-controller. Three low cost MEMS accelerometers (Bosch BMA-150) are attached to the node and capable of sampling at 1500 Hz (bandwidth 750 Hz).

3.1 *Laboratory testing*

A steel reinforced concrete beams was manufactured with a similar geometry to those on the Sydney Harbour Bridge where an I-beam (UB 200-18) was embedded inside the concrete as shown in the cross section of Figure 3. The length of the specimen was 2000 mm, the width was 1000 mm and the depth was 375 mm. After poring the concrete (32 Mpa), the specimen was left to cure for at least 28 days (according to the Australian Standard) at room temperature before testing. The specimen was fixed at one end using a steel bollard to form a cantilever, where 400 mm along the length of the beam were fully clamped as shown in Figure 3 and Figure 4. In addition, a support was placed at 1200 mm away from the tip to avoid any cracking occurring in the specimen under self-weight.

The input excitation was modelled as filtered Gaussian white noise (stochastic process with Gaussian distribution) with a mean of 0 and a standard deviation of 0.333.The modelled noise was fed into the shaker that was fixed in the middle of the specimen and toward the tip, as shown in Figure 4(b). The Gaussian white noise runs for a duration of 20 minutes. The data are collected continuously at a sampling rate of 500 Hz and bandwidth of 250 Hz.

After testing the benchmark, a crack was introduced into the specimen in the location indicated in the Figure 3 (a) and Figure 4 (c) using a cutting saw. The length of the cut was increased gradually from 75 mm to 270 mm as shown in Figure 3(c-f), and the depth of the cut was fixed to 50 mm. The data were collected from a sets of 3 single accelerometers (PCB 352C34) placed on the tip of the joint and they are referred to as sensor 1, sensor 2 and sensor 3 as shown in Figure 4(c). Following every damage case, the Gaussian white noise excitation was applied again and the vibration data were collected in a similar fashion to the benchmark.

A description of the damage cases is detailed in Table 1.

Table 1. Description of tested cases.

Case	Damage size
Benchmark	--
Damage 1	75 mm x 50 mm
Damage 2	150 mm x 50 mm
Damage 3	225 mm x 50 mm
Damage 4	270 mm x 50 mm

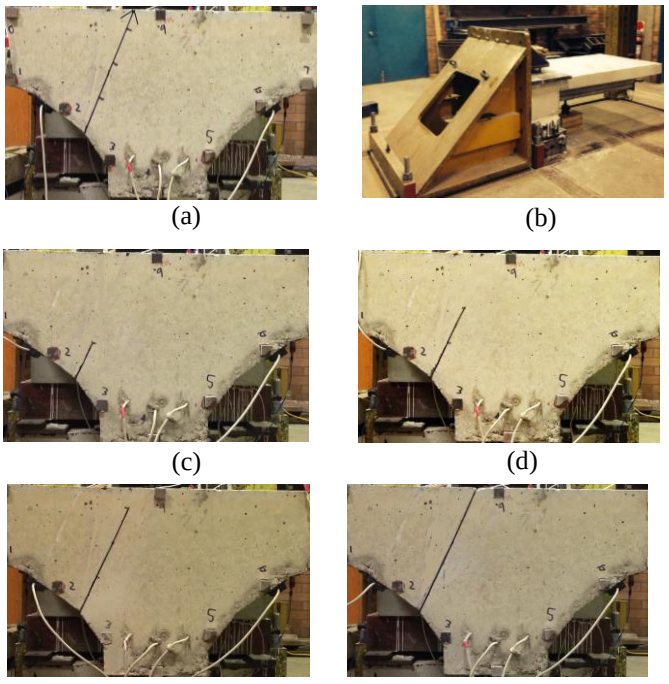

Figure 3. Boundary condition and loading of the beam specimen: (a) intact with the arrow indicating the direction of the cut, (b) clamping of the specimen, (c) 75 mm cut, (d) 150 mm cut, (e) 225 mm cut and (f) 270 mm cut.

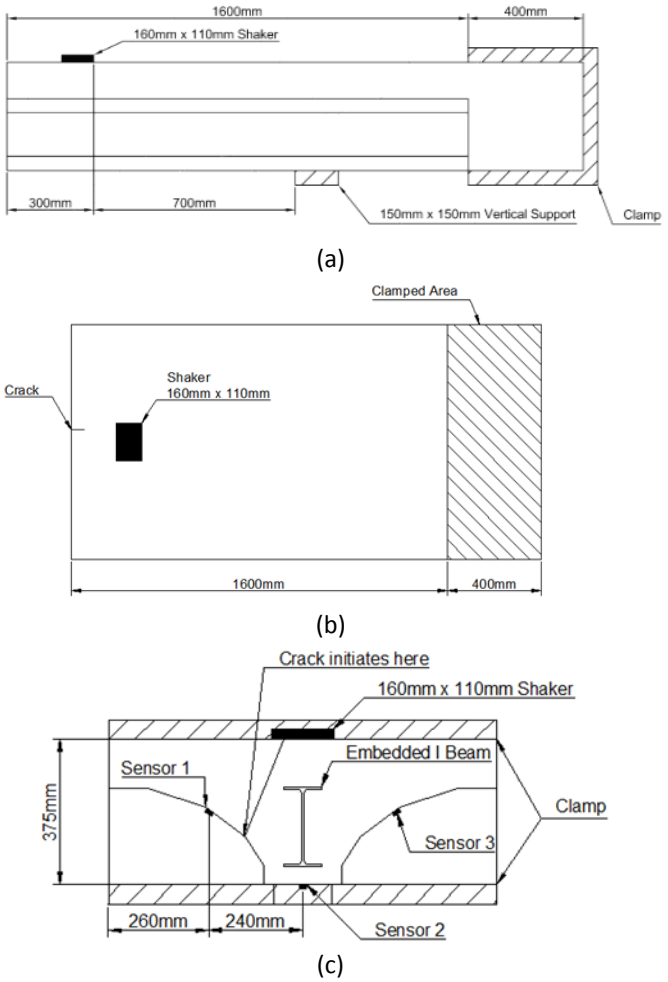

Figure 4. Detailed geometry of the beam section (a) elevation view, (b) plan view and (c) cross sectional view.

3.2 *Field trial*

For the current case study, 6 instrumented jack arches were considered for this analysis (similar dimensions to Figure 4). They are named Joint 1 to Joint 6 moving from north to south following the direction of the traffic, shown in the schematic of Figure 5. These joints are located on the eastern side of the bridge underneath lane 7 (Bus lane – Figure 5(a)) near the north pylon. Analysed data are collected from tri-axial accelerometer mounted on the base of each joint (illustrated in Figure 5 (b)).

The data were collected after the vehicles (usually buses) drive over the deck where the nodes are located. A pre-set threshold was used to trigger the recording on the node. The data were collected during the period from August to October in 2012. During this time a known crack existed on joint 4 while all the others were in good conditions. Each node (after it is triggered) records for a period of 1.5 seconds at a sample rate of 400 Hz. Later, Joint 4 was repaired in February 2013 and another set of data was collected on the 10th of April 2014. In this case, two sets of data were available for analysis: (a) Joint 4 damaged and the rest of joints are healthy and (b) all joints healthy.

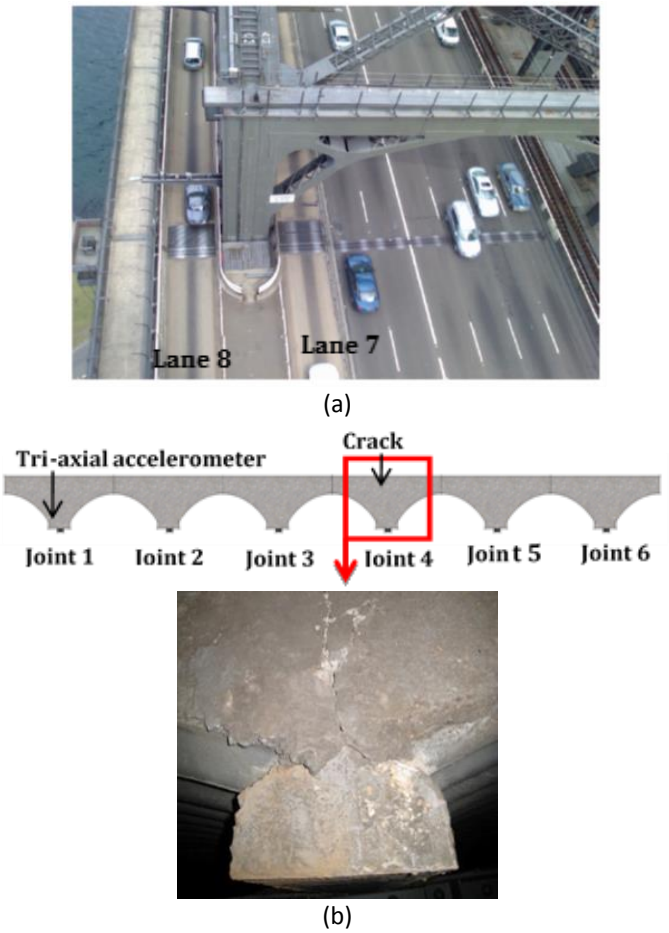

Figure 5. Schematic of the evaluated joints (a) location of testing and (b) sensor configuration.

Before proceeding into the analysis and discussion section, it is worth mentioning that although the PCB 352C34 has a much wider measurement range in comparison with the Bosh BMA150, however the amount of g-force acting on the bridge due to traffic loading can hardly exceed ± 2g which is within the measurement range of the Bosh BMA150. In addition, the Bosh BMA150 has a resolution up to 4 mg within the ± 2g measurement range (BOSH 2015;PCB 2015). Furthermore, the BMA150 has an output noise of $0.5\ mg/\sqrt{Hz}$ and a programmable bandwidth up to 1500 Hz and therefore capable of capturing ambient vibration within the 1500 Hz range.

4 ANALYSIS AND DISCUSSION

4.1 *Results: laboratory testing*

Using the healthy events that were collected during the laboratory testing, 50 events were chosen randomly to establish the ARX model for the intact state. After the standardizing process is completed, an order selection was performed to determine the best order for the AR model. The AIC was calculated for different orders varying from 1 to 50. It was determined that an order of 17 results in the most negative value of AIC as shown in Figure 6 which indicate a larger maximum likelihood and a lower order, therefore 17 will be selected as an order for the benchmark AR model.

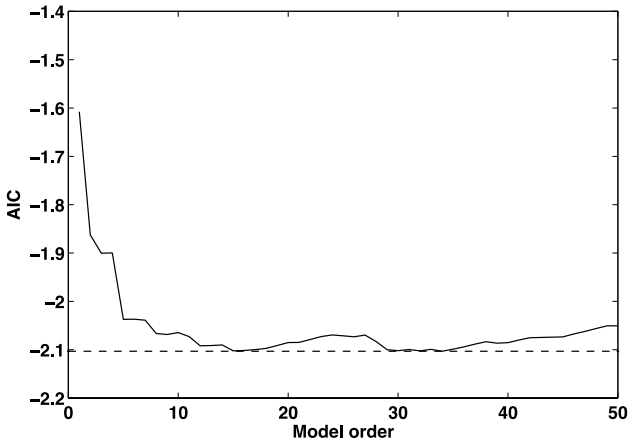

Figure 6. Order selection for the benchmark AR model based on the AIC.

Following the order selection of the AR mode, the coefficients of the polynomial of the AR model were calculated based on the Yule Walker method, the Φ_{AR} polynomial was calculated to be:

$$\Phi_{AR}(q) = 1 - 0.8102q^{-1} + 0.5275q^{-2} + 0.2242q^{-3} - 0.4829\ q^{-4} + 0.0687q^{-5} - 0.0705q^{-6} + 0.0614q^{-7} + 0.1356\ q^{-8} - 0.1174q^{-9} + 0.05335q^{-10} - 0.0014\ q^{-11} - 0.0499q^{-12} + 0.0487\ q^{-13} + 0.00093466q^{-14} - 0.0721\,q^{-15} + 0.1407q^{-16} - 0.1634q^{-17} \quad (7)$$

The fitting between the measured data and AR model was examined, shown in Figure 7, and a fit of 66.7 % was achieved. At this stage the effect of the ambient excitation have not been considered appropriately in this model, therefore the full dynamic characteristics of the system have not been captured. Furthermore, the calculated error is not a random value, which means that there are some correlations that have not been extracted (coloured noise). The error from the AR model may be attributed to the disturbance (external effects) coming into the system, therefore this error was assumed to cause the disturbance input (U) into the function $\boldsymbol{\Theta_{ARX}(q)}$ (Figure 1) of the ARX model. Subsequently, the coefficients for the ARX model can be determined using the Yule Walker method since the two inputs into the model including the previous acceleration data and the current excitation (error resulted from the AR model) are known. Note that the sum of the order of $\boldsymbol{\Phi_{ARX}}$ and $\boldsymbol{\Theta_{ARX}}$ should be less than the order of $\boldsymbol{\Theta_{AR}}$. The two polynomial equations of the ARX model are determined to be:

$$\Phi_{ARX}(q) = 1 - 0.7457\ q^{-1} + 0.7303\ q^{-2} + 0.4061\ q^{-3} - 0.4268\ q^{-4} + 0.1090q^{-5} + 0.1766q^{-6} - 0.2148\ q^{-7} + 0.1002\ q^{-8} \quad (8)$$

and

$$\Theta_{ARX}(q) = 0.9975 + 0.0656\ q^{-1} + 0.2543\ q^{-2} + 0.3526\ q^{-3} + 0.1957\ q^{-4} + 0.1090\,q^{-5} - 0.0158q^{-6} + 0.1714\,q^{-7} - 0.0148\ q^{-8} \quad (9)$$

Based on the comparison between the measured data and the ARX model, shown in Figure 8, the fitting has improved by approximately 6.5%.

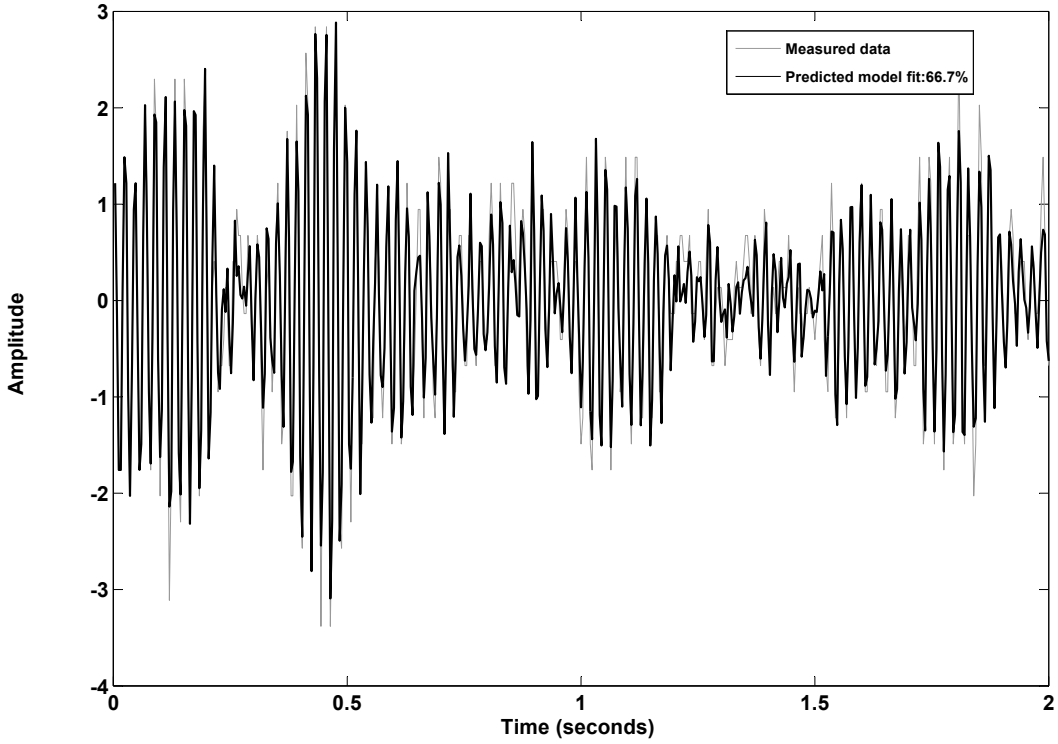

Figure 7. Measured output and predicted model for an undamaged case with AR(17) model.

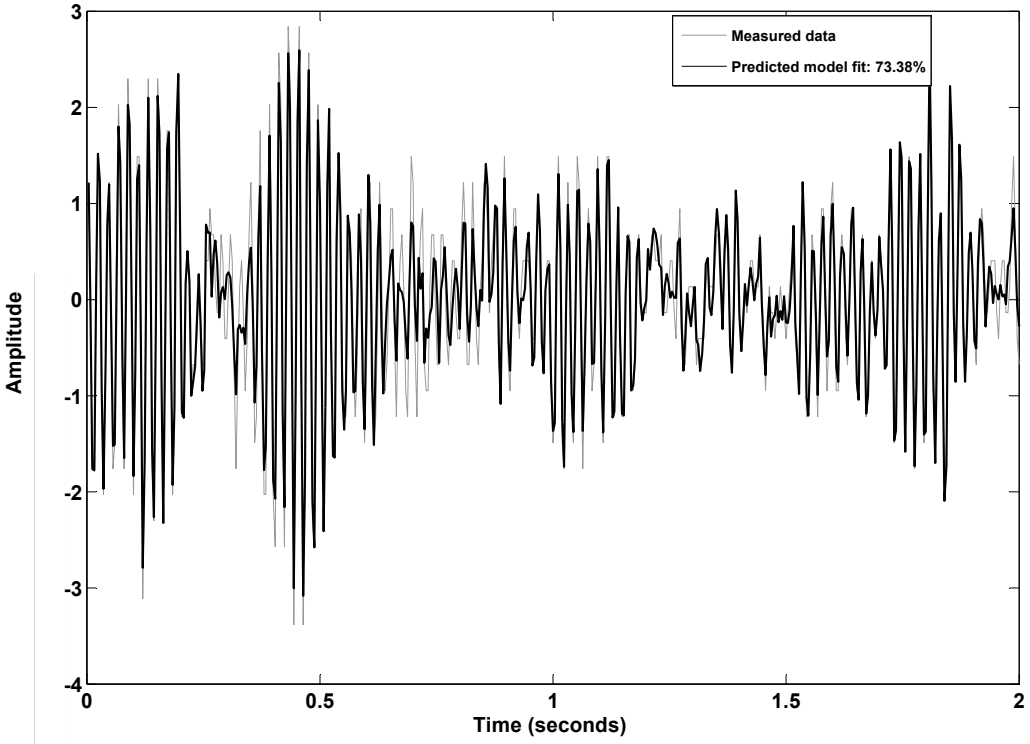

Figure 8. Measured output and predicted model for an undamaged case with ARX model using Sensor 2 data.

Most importantly in this situation is that the residual error from the ARX model is now normally distributed, which means it is now an independent pattern and has no effect on the structural dynamic function, as it appears in Figure 9.

The process was repeated for Sensor 1, Sensor 2 and Sensor 3 to establish the AR and ARX benchmark models.

After finalising the model for the benchmark, the data collected from the healthy state were tested in order to ensure that they fit well into the established

ARX model and that DI fallout in the expected range. The process for testing starts by creating a AR model for every time series collected (event) from the accelerometers, ensuring the new model has the same order as the benchmark, and then the residual error (e) from the AR model is calculated and fed back into the ARX benchmark model (established earlier) to obtain the ARX residual error (ϵ). Finally, the standard deviation for the ARX residual error is calculated for the testing data. Afterward, the DI is calculated as defined in Equation 5. The same procedure is repeated after the crack was gradually introduced and once more the DI is calculated for the data collected after the damage.

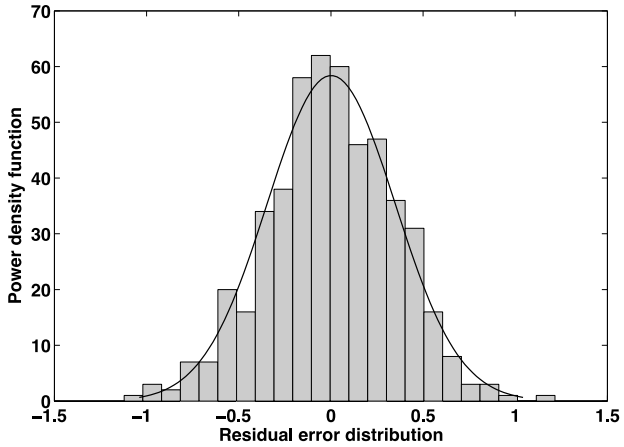

Figure 9. Residual error with Gaussian distribution using the benchmark data (ARX) using sensor 2 data.

Damage 4 was considered to illustrate the sensitivity of the approach to detect damage. The DI was calculated using the data collected from Sensor 2 for both healthy and damaged case as it appears in Figure 10 (a). The mean of the scattered data was calculated for easier interpretation. For this case 50 events were able to provide an accurate estimate of the mean, which resulted in a uniform standard deviation when the number of events was further increased. When the structure is intact, the mean value obtained for the DI was calculated to be 1.6, while the existence of damage resulted in an increase of the DI to 2.2, which is about 27% increase. It was also observed that the events received from the damaged states are well separated from the intact state and can be easily identified.

Moreover, the effect of the extent of damage was investigated. Based on data collected from Sensor 2 and Sensor 3, the first damage case (75 mm) resulted in an increase in the DI. However, when the damage size was further increased, it was noticed that the DI dropped slightly and then further increased for damage case 3. On the other hand, using the data collected from sensor 1, the DI continues increasing for the following the three damage cases and suddenly dropped when the damage size reached 270 mm. Based on the above, it was observed that the increase in the damage size changes the dynamic characteristics, however it does not follow any particular pattern, as shown in Figure 10 (b).

In addition, it was observed that the location of the sensor did not influence the DI in regular trend. The DI was highest when calculated using the data captured with Sensor 3 which is furthest away from the crack, while the DI calculated based on the data captured with Sensor 1 and Sensor 2 were within the same range.

The results in Figure 10 (a) indicated that the location of the sensor as well as the severity of damage are not directly proportional to the DI calculated.

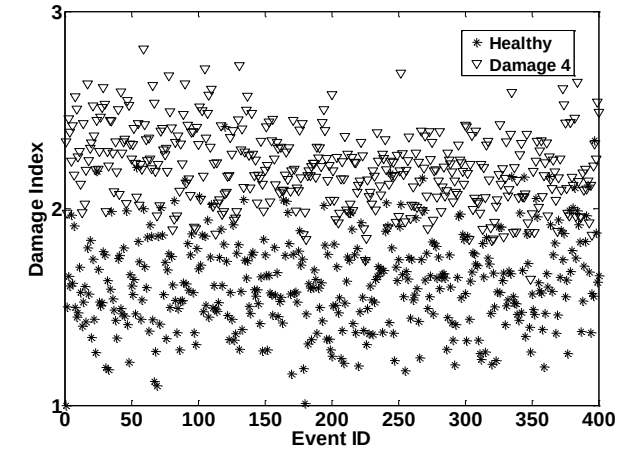

(a)

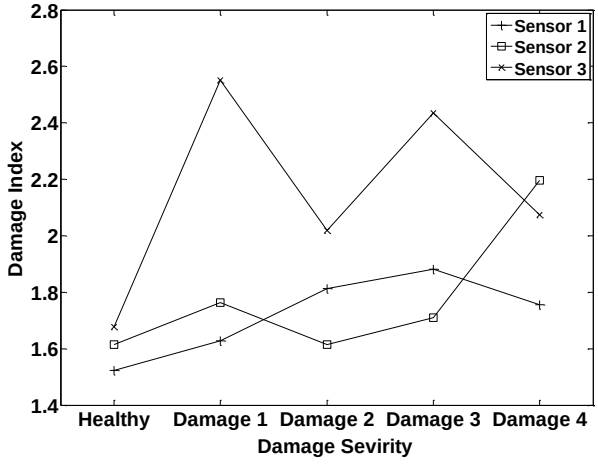

(b)

Figure 10. (a) Separation of the benchmark and damaged data using the ARX residual errors based on the data collected Sensor 2 (b) effect of damage extent on the DI.

4.2 *Results: field trial*

With the data collected in the laboratory, the healthy and the damaged condition were available for analysis. While with the field trial the data are only available for one state of the structure, however what make this analysis valuable is that one of the joints (Joint 4) had a crack, along the front face and the crack propagated toward the surface of the deck, while the other joints were intact. The cracked joined was later repaired in February 2013, therefore two sets of data were obtained for the healthy case and the damaged cased. As all the joints are very similar in geometry (the dynamic characteristic may differ slightly due to the slight change in the boundary conditions), any of the healthy joints can be used to establish the benchmark ARX model. For this particular case, Joint 1 was used to form the benchmark model.

After forming the benchmark model, the data collected from all the joints can be tested, as described in the previous section, to calculate the DI. Figure 11 (a) summarizes the data obtained from the bridge, once more the healthy and the damaged data can be easily separated, before and after the repair has occurred on Joint 4. It appears that all the joints beside Joint 4 has a mean value around 2.2, while for Joint 4 the mean value increased to above 7 for the damaged case and then dropped to 2 after the repair, as shown in Figure 12.

As it appears from Figure 12 that it is very difficult to obtain a DI of 1 when testing the healthy joints on the bridge, although theoretically they should be. This is mainly due to the nature of excitation, unless the excitation is Gaussian white noise, a DI of 1 is difficult to achieve. When the excitation is coloured noise, which is the case on the bridge, some extreme loading highly influences the construction of the AR model resulting in a deviation of the DI from 1.

Both laboratory and field testing indicate that the AR-ARX model developed in this study has a high sensitivity to small structural changes, such as cracking.

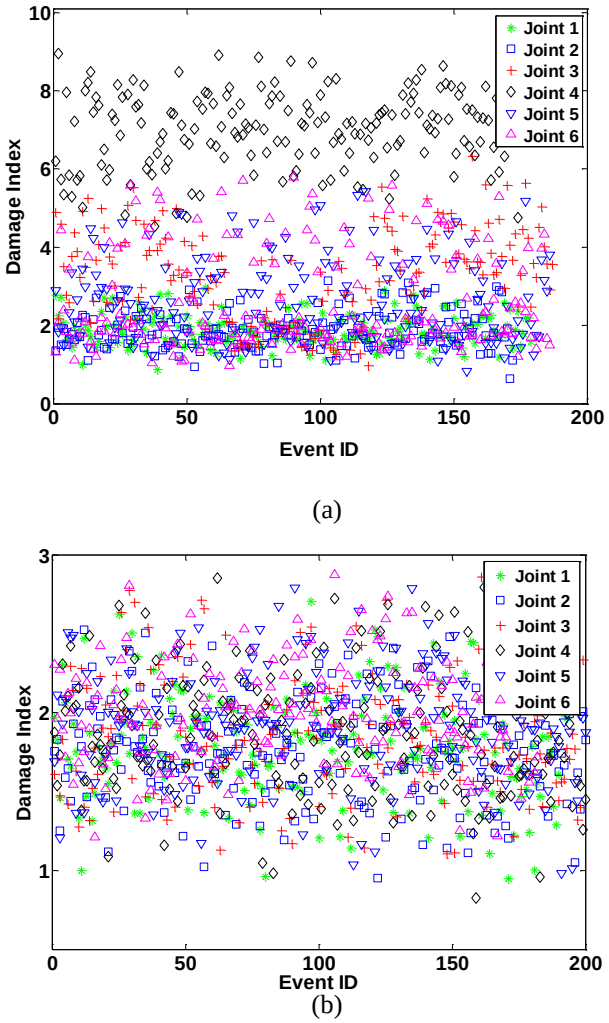

Figure 11. Separation of the benchmark and damaged data using the ARX residual errors: (a) before repair and (b) after repair.

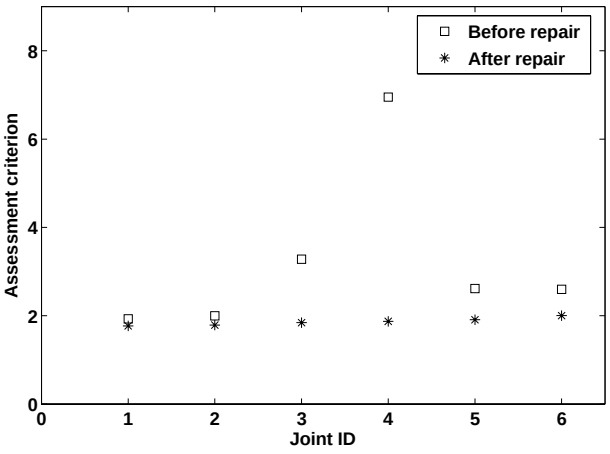

Figure 12. Mean value calculated based on the DI.

5 CONCLUSIONS AND FUTUE WORK

In this paper, a vibration based method for damage detection was demonstrated using time series analysis. An AR-ARX two-staged model was adopted to identify any structural change based on the re-

sidual errors obtained from the ARX model. Field trial and laboratory testing were performed to validate the approach, the method has shown a high potential to identify cracking in concrete structures.

Various factors related to implementation were discussed including the sample size, the training data size and the testing scheme.

Despite the excitation on the Sydney Harbour Bridge cannot perfectly behave like Gaussian white noise that still can give a good indication of the existence of damage. Interestingly, when the damaged joint was repaired, the data collected (after repair) fitted well into the trained model. Therefore, this approach has the ability to assess the repaired regions in the bridge.

Based on the laboratory testing there was no clear pattern relating the location of the sensor to the resulting damage index. However, it was clear that despite the location of the sensor we were capable of identifying the presence of damage.

Future work will involve the development of more sophisticated experiments to understand the sensitivity of the approach to early cracking due to fatigue and have the ability to define a proper threshold to indicate damage/cracking. The authors will also focus on using a classification algorithm to identify different levels of damage. Furthermore, more work is needed to deal with de-colouring the noise in order to improve the robustness of this method.

6 REFERENCES

Bosh, S., *Bma150,* 2015, BOSH, 22nd of January, 2015,<https://www.bosch-sensortec.com/en/homepage/products_3/3_axis_sensors/acceleration_sensors/bma150_4/bma150>.

Brockwell, P. & Davis, R., *Introduction to Time Series and Forecasting,* 2002, Springer.

Da Silva, S., Dias Junior, M. & Lopes Junior, V., "Structural Health Monitoring in Smart Structures through Time Series Analysis", *Structural Health Monitoring,* Vol. 7, No.3, 2008, pp. 231-244.

De Lautour, O. R. & Omenzetter, P., "Damage Classification and Estimation in Experimental Structures Using Time Series Analysis and Pattern Recognition", *Mechanical Systems and Signal Processing,* Vol. 24, No.5, 2010, pp. 1556-1569.

Farrar, C. R. & Worden, K., 'Damage-Sensitive Features', In *Structural Health Monitoring*2012, John Wiley & Sons, Ltd, pp. 161-243.

Fugate, M. L., Sohn, H. & Farrar, C. R., "Vibration-Based Damage Detection Using Statistical Process Control", *Mechanical Systems and Signal Processing,* Vol. 15, No.4, 2001, pp. 707-721.

Gul, M. & Catbas, F. N., "Structural Health Monitoring and Damage Assessment Using a Novel Time Series Analysis Methodology with Sensor Clustering", *Journal of Sound and Vibration,* Vo;. 330, No.6, 2011, pp. 1196-1210.

Mei, Q. & Gul, M., 'An Improved Methodology for Anomaly Detection Based on Time Series Modeling', In (Eds, Catbas, F. N., Pakzad, S., Racic, V., Pavic, A. &Reynolds, P.), *Topics in Dynamics of Civil Structures, Vol 4,* 2013, Springer New York, pp. 277-281.

Mustapha, S., Ye, L., Wang, D. & Lu, Y., "Debonding Detection in Composite Sandwich Structures Based on Guided Waves", *AIAA journal,* Vol. 50, No.8, 2012, pp. 1697-1706.

Pcb, P., *Model: 352c34,* 2015, PCB Group, 22nd of January, 2015,<http://www.pcb.com/Products.aspx?m=352C34>.

Peng, Z. K., Lang, Z. Q., Wolters, C., Billings, S. A. & Worden, K., "Feasibility Study of Structural Damage Detection Using Narmax Modelling and Nonlinear Output Frequency Response Function Based Analysis", *Mechanical Systems and Signal Processing,* Vol. 25, No.3, 2011, pp. 1045-1061.

Silva, S. D., Dias Júnior, M. & Lopes Junior, V., "Damage Detection in a Benchmark Structure Using Ar-Arx Models and Statistical Pattern Recognition", *Journal of the Brazilian Society of Mechanical Sciences and Engineering,* Vol. 29, 2007, pp. 174-184.

Sohn, H. & Farrar, C. R., "Damage Diagnosis Using Time Series Analysis of Vibration Signals", *Smart Materials and Structures,* Vol. 10, No.3, 2001, pp. 446-451.

Sohn, H., Farrar, C. R., Hunter, N. F. & Worden, K., "Structural Health Monitoring Using Statistical Pattern Recognition Techniques", *Journal of Dynamic Systems, Measurement, and Control,* Vol. 123, No.4, 2001, pp. 706-711.

Thanagasundram, S. & Schlindwein, F. S. 2006 In *Proceedings of ISMA2006 Noise and Vibration Engineering Conference*, pp. 3531-3546.

Yao, R. & Pakzad, S. N., "Autoregressive Statistical Pattern Recognition Algorithms for Damage Detection in Civil Structures", *Mechanical Systems and Signal Processing,* Vol. 31, 2012, pp. 355-368.